Microstripes for transport and separation of magnetic particles

Marco Donolato,[1,2] Bjarke Thomas Dalslet,[1] and Mikkel Fougt Hansen[1]
[1]*Department of Micro- and Nanotechnology, Technical University of Denmark, DTU Nanotech, Building 345B, DK-2800 Kongens Lyngby, Denmark*
[2]*CIC nanoGUNE Consolider, Tolosa Hiribidea 76, 20009 San Sebastian, Spain*

(Received 1 February 2012; accepted 28 March 2012; published online 13 April 2012)

We present a simple technique for creating an on-chip magnetic particle conveyor based on exchange-biased permalloy microstripes. The particle transportation relies on an array of stripes with a spacing smaller than their width in conjunction with a periodic sequence of four different externally applied magnetic fields. We demonstrate the controlled transportation of a large population of particles over several millimeters of distance as well as the spatial separation of two populations of magnetic particles with different magnetophoretic mobilities. The technique can be used for the controlled selective manipulation and separation of magnetically labelled species. © *2012 American Institute of Physics*. [http://dx.doi.org/10.1063/1.4704520]

The selective manipulation of bioparticles in lab-on-a-chip systems is attracting a large interest due to the need to focus and separate target bioentities.[1,2] Devices based on dielectrophoresis, which rely on locally generated electrical fields, have been promoted for, e.g., selective focusing,[3] filtering,[4] and travelling wave transportation[5] of bioparticles in a liquid flow. The size separation of micron sized particles has also recently been demonstrated.[6] These devices, generally label-free, rely on integrated electrodes and put requirements on the ionic content of the sample liquid, a condition that can limit the range of compatible biological entities.[1]

Devices for bioparticle manipulation by magnetic forces generated by external magnetic structures or by on-chip magnetic structures in combination with externally applied magnetic fields have recently emerged for flow-sorting or for manipulation of particles in a stagnant solution.[2] These methodologies are not sensitive to the sample chemistry and do not require electrical contacts to the chip. However, they are not label-free as the target bioparticles have to be magnetically labelled. Devices based on magnetic manipulation are attractive due to the generally lower complexity of the chip and the chip packaging, their low requirements for the sample chemistry and due to the potentially infinite separation efficiency when magnetically labelled species are separated from unlabelled non-magnetic species.

In the literature, the precise manipulation of a limited number of magnetically tagged biomolecules and cells on the nanometer scale has been demonstrated by the controlled injection and motion of domain walls in soft magnetic micro- and nanowires.[7,8] The magnetic transportation of a larger quantity of particles has been demonstrated by use of periodic arrays of soft magnetic ellipsoids[9,10] and of hard magnetic circular disks.[11,12] The latter authors have also studied the particle transportation as function of the frequency f of the harmonically varying applied magnetic field and have demonstrated theoretically and experimentally that a particle will not be transported when f exceeds a critical value that depends on the magnetic moment and the hydrodynamic size of the particle.[11] The manipulation of particles using the controlled motion in domain walls in continuous magnetic thin films has also been demonstrated for bismuth-substituted ferrite garnet films[13] and for exchange-biased thin films magnetically patterned into parallel stripes by ion irradiation,[14] but these studies did not demonstrate a selective particle manipulation.

In this paper, we present and demonstrate a new technique for creating an on-chip conveyor for magnetic particles using exchange-biased permalloy microstripes produced with a single lift-off step. A moving, spatially periodic potential energy landscape, capable of transporting

magnetic particles is created by choosing a distance between the stripes smaller than their width and by applying an appropriate sequence of external magnetic fields. A large population of magnetic particles can then be moved in a controlled fashion without the requirement of any liquid flow. This approach differs from the methods relying on domain wall motion in continuous films presented above, as it relies on a fixed magnetic domain geometry defined by the stripe geometry, and as it requires neither exotic materials such as the ferrite garnet films[13] nor the creation of artificial antiparallel domains through ion-irradiation.[14] The device presented here requires only a simple structuring by lift-off or etching of a standard thin film material, which can be deposited on any substrate. In addition to the transportation of a single species of magnetic particles, we show that the device can be used to separate at least two populations of magnetic particles with different magnetophoretic mobilities. This technique has the advantage over periodic arrays of circular or ellipsoidal microstructures that all particles have the same initial conditions, as the magnetic energy does not vary along the *y*-direction. This can potentially improve the separation efficiency and furthermore, as we will show, it reduces clustering of the magnetic particles due to magnetic interactions.

Figure 1(a) shows a top view schematic of the device. A series of exchange-biased permalloy stripes 6 mm long and 10 μm wide with a separation of 2.5 μm (giving a stripe period of $P = 12.5$ μm) have been patterned on a Si/SiO_2 surface. The stack with the nominal composition $Ta(5)/Ni_{80}Fe_{20}(20)/Ir_{20}Mn_{80}(20)/Ta(5)$ (thicknesses in nm) was sputtered in a K. J. Lesker Co. model CMS 18 magnetron sputtering system and defined by lift-off. During deposition, a magnetic flux density of 20 mT was applied in order to define an easy magnetization direction of the $Ni_{80}Fe_{20}$ layer in the negative *x*-direction. Subsequently, a protective coating of SiO_2 with a thickness of 100 nm was sputter deposited to prevent corrosion of the stripes. Figure 1(b) shows the easy axis hysteresis loop measured on a patterned device using a LakeShore model 7407 vibrating sample magnetometer. The exchange bias field obtained from the hysteresis loop is $\mu_0 H_{ex} = -5.5$ mT, where μ_0 is the permeability of free space and the negative sign reflects a preferred magnetization direction along the negative *x*-direction. For the experiments with magnetic beads, the chip was mounted in a cavity in a microfluidic chamber formed by laser ablation in a polymethylmethacrylate (PMMA) plate. Subsequently, a microscope slide cover slip lid was attached using double-adhesive tape. The device parts are illustrated in Fig. 1(c), while their assembly is sketched in Fig. 1(d). During experiments, the system was placed in a home built electromagnet that could provide magnetic fields in the *x*- and

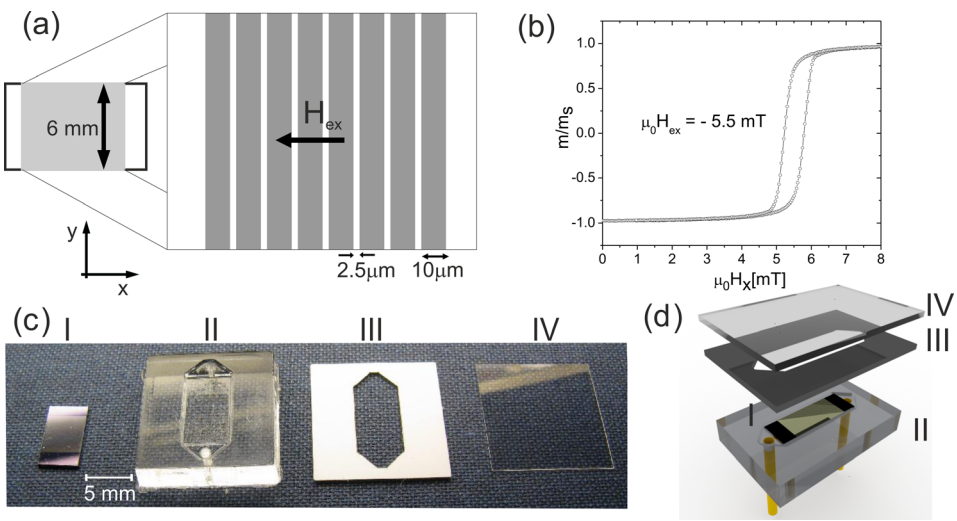

FIG. 1. (a) Schematic of the device indicating the relevant geometric dimensions. (b) Magnetic hysteresis loop on the patterned sample measured along the *x*-direction. (c) The chip (III) with the chip holder (IV), the adhesive tape (II) and the glass lid (I) prior to assembly of the microfluidic system. (d) Schematic of the assembly of parts (I)-(IV) of the fluidic system (enhanced online). Video M1 [URL: http://dx.doi.org/10.1063/1.4704520.1]

z-directions. Movies were recorded using a Leica MZ FLIII stereo microscope equipped with a Sony DFW-X710 camera.

Figure 2 illustrates a method capable of reversibly transporting magnetic particles from one stripe to the other by changing the applied field in the y-plane in four steps.

The force experienced by a magnetic particle in a magnetic field can be expressed as[15]

$$\mathbf{F} = \mu_0 V \chi (\mathbf{H} \cdot \nabla)\mathbf{H}, \tag{1}$$

where V is the volume of the magnetic particle, χ is the effective magnetic particle susceptibility, and $\mathbf{H}$ is the magnetic field in the absence of the particle. For a particle with uniform susceptibility, we can use the identity $(\mathbf{H} \cdot \nabla)\mathbf{H} = \frac{1}{2}\nabla H^2$ and $\mathbf{F} = -\nabla U$, where U is the potential magnetic energy of the particle, to write

$$U = -\frac{1}{2}\mu_0 V \chi H^2. \tag{2}$$

By choosing a proper sequence of applied external magnetic fields, it is possible to shift the energy minimum for a magnetic particle and hence to shift its position to create an effective particle transportation. The top row of Fig. 2 shows the normalized energy $U/(V\chi)$ calculated using Eq. (2) at a distance of 1 μm from the substrate for $Ni_{80}Fe_{20}$ stripes having the same geometrical dimensions as the real sample with a magnetization $\mu_0 M_x = -1.1$ T. These curves were obtained using COMSOL MULTIPHYSICS (COMSOL A/S, www.comsol.com). When no external field is applied, the stripes present equally attractive magnetic poles on both sides. When a positive magnetic field $H_{app,z}$ is applied in the z-direction, the potential energy landscape shows a minimum near the North pole and a maximum near the South pole of each stripe where the stray field from the stripe is parallel and antiparallel to the applied field, respectively. Accordingly, the particles will position themselves on one side of the stripes, as shown in Fig. 2(a) where the curve has been calculated for $\mu_0 H_{app,z} = 5$ mT. Applying an additional field in the positive x-direction, i.e., parallel to the stray field over the middle of the stripe, shifts the energy minimum toward the centre of each stripe as shown in Fig. 2(b) calculated for $\mu_0 H_{app,z} = 2.5$ mT and $\mu_0 H_{app,x} = 5$ mT. Reversing the sign of $\mu_0 H_{app,z}$, the minimum shifts toward the other side of each stripe (Fig. 2(c)) and when $\mu_0 H_{app,x}$ is removed, the minimum is localized near the South pole of the stripe (Fig. 2(d)). When the initial field configuration is restored, the particles move toward the nearest North pole, which is now the one of the next stripe, as shown in Fig. 2(e)). The particle motion can then continue toward the positive x-direction by repeating the sequence. The particle motion can also be reversed by reversing the field sequence.

The images on the bottom row of Fig. 2 show magnetic particles positioned on the stripes in the same field configurations as those simulated. The images show particles in the positions corresponding to the calculated energy minima and hence validate the calculations. In these

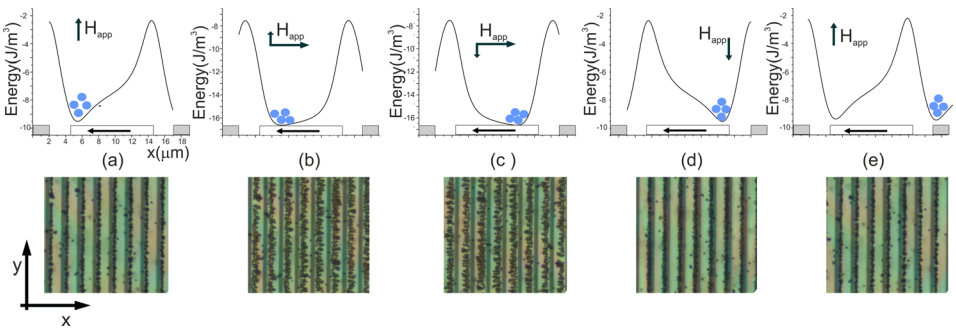

FIG. 2. The top row shows the normalized energy calculated using COMSOL at a distance of 1 μm from the substrate over a single stripe surface for ($\mu_0 H_{app,x}$ [mT], $\mu_0 H_{app,z}$ [mT]) = (0, 2.5), (5, 2.5), (5, −2.5), (0, −2.5) and (0, 2.5) in parts (a)–(e), respectively. The bottom row shows the corresponding experimental images (enhanced online). Video M2 [URL: http://dx.doi.org/10.1063/1.4704520.2]

experiments, a dilute suspension of 1.05 μm magnetic beads (Carboxyl Magnetic Particles, Spherotec, Inc., Lake Forest, IL, USA) was injected in the fluidic system, and a field of 7 mT was initially applied along the negative x-direction to enhance the trapping of the beads between the stripes. Then, by manually stepping through the field sequence, the magnetic beads were transported along the stripes (see video M1). As can be observed from the experimental data, clustering of magnetic beads is minimized, because the beads are localized along a line oriented along the stripes and magnetized perpendicular to the stripes so they repel each other by magnetic dipole interactions.

The velocity Δv of a magnetic particle relative to the carrier fluid under the action of a magnetic field gradient can be expressed as[14]

$$\Delta v = \mu_0 \xi \nabla (H^2), \tag{3}$$

with the magnetophoretic mobility

$$\xi = \frac{V\chi}{12\pi\eta r_h}, \tag{4}$$

where r_h is the hydrodynamic radius of the particle, η is the viscosity of the medium, and we have assumed Stokes drag and that the medium is non-magnetic. For a magnetic bead, where the hydrodynamic radius is identical to the magnetic radius r, Eq. (4) simplifies to

$$\xi_{\text{bead}} = \frac{r^2\chi}{9\eta}. \tag{5}$$

For a long period (low frequency) of the external field sequence the energy potential moves slower than Δv, and the particles will move with the potential energy minimum. At a frequency above a threshold value defined by the magnetophoretic mobility, the particles move too slowly to follow the potential energy minimum and will not be able to transfer between the stripes. Thus, a translating energy potential can be used for separating particles with different magnetophoretic mobilities as proposed by Yellen *et al.*[11]

To demonstrate the ability to separate particles with different magnetophoretic mobilities, we carried out experiments with two different bead types: carboxylic acid coated M-280 beads with a diameter of 2.8 μm and streptavidin coated MyOne beads with a diameter of 1 μm both from Invitrogen A/S. Using the measured low-field effective magnetic bead susceptibilities from Ref. 16 in Eq. (5), we find that the magnetophoretic mobility of the M-280 beads is about four times that of the MyOne beads. This implies that the M-280 beads will move at about four times the speed of the MyOne beads when driven by the same field gradient. In the experiments, we injected a mixed suspension with identical mass concentrations of the two bead types into the fluidic system. To reduce the non-magnetic interactions between the beads and the surface, we followed the protocol described in Ref. 7. After bead injection, we applied the previously presented sequence of fields where each step in the field sequence had a duration of t_f and studied the bead transportation as function of t_f. We define the maximum transport velocity for a certain bead type as the maximum value for which at least 75% of the beads optically monitored in a 500 μm $\times$ 500 μm area can follow the translating potential. When t_f was lower than about 80 ms, the majority of both bead types could not follow the energy minimum and oscillated back and forth on a single stripe.

In a sequence of experiments, we measured maximum net transportation velocities $v_b \equiv P/(4t_f)$ of (40 ± 4) μm/s for the M-280 beads and (12 ± 3) μm/s for the MyOne beads. These results are in agreement with the ratio of four between the magnetophoretic mobilities of the two bead types. These velocities can be further increased by optimization of the field sequence and its timing.

Figures 3(a) and 3(b) show a part of two frames from the video M2 that demonstrate the selective transportation of M-280 and MyOne beads. In the first frame (Fig. 3(a)), both beads

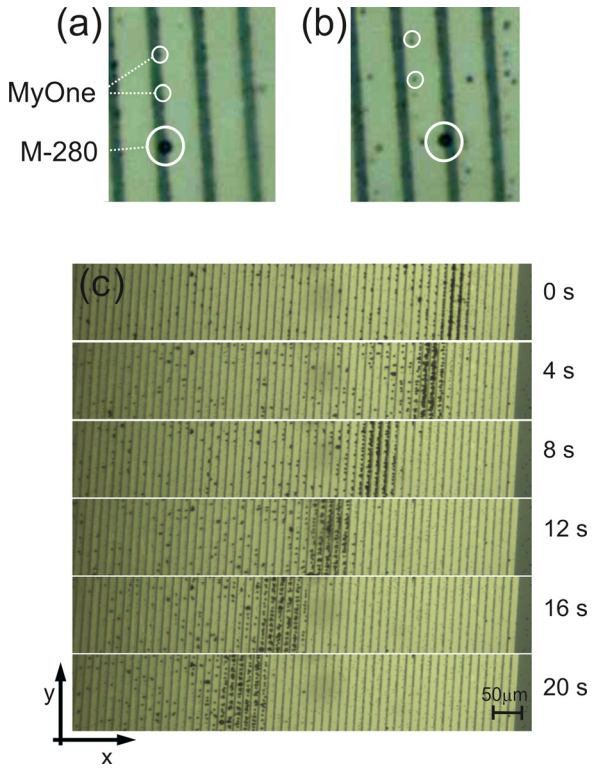

FIG. 3. Parts (a) and (b) show two frames from the video M2 corresponding to steps (a) and (d) in Fig. 2 for M-280 and MyOne beads with $t_f = 180$ ms. Only the M-280 beads are able to cross the stripe (light color). (c) Sequence of frames from the video M3 where a field sequence with $t_f = 140$ ms is applied. The M-280 beads are translated in the negative x-direction, whereas the MyOne beads (small dots mainly visible on the left side) are left behind (enhanced online). Video M3 [URL: http://dx.doi.org/10.1063/1.4704520.3]

type are trapped at the stripe side by a positive field $H_{app,z}$. After the four field steps corresponding to Figs. 2(a)–2(d) with $t_f = 180$ ms, the M-280 beads reach the other side of the stripe, whereas the MyOne beads are still close to the center of the stripe (see Fig. 3(b)). When the sign of $H_{app,z}$ is reversed, corresponding to Fig. 2(e), the MyOne beads are translated back to their starting position, whereas the M-280 beads will be further transported to the next stripe in the subsequent field step.

Figure 3(c) and video M3 show a sequence of frames where a large amount of M-280 and the MyOne beads are separated using the exchange-biased stripe device. Prior to acquisition of the shown images, the beads were transported towards the right in Fig. 3(c) for a number of cycles using $t_f = 300$ ms. When beads reached the last stripe, they oscillated back and forth between the two sides of the stripe. The sequence of frames in Fig. 3(c) and the supplementary video M3 show the behaviour after the field sequence is reversed and t_f is reduced to 140 ms. This value corresponds to $v_b \approx 20$ μm/s, which is above the maximum bead velocity for the MyOne beads but well below the maximum velocity of the M-280 beads. Hence, most of the MyOne beads are unable to follow the translating energy minima and are left behind while almost all of the M-280 beads are being transported. During the transportation, the band corresponding to the M-280 beads slightly expands due to variations in the magnetophoretic mobility of the beads and/or non-magnetic interaction with the substrate.

In conclusion, the described device works as a microscopic conveyor for the controlled transport of a large amount of magnetic particles for up to mm distances. The presented structures impose identical initial conditions for the particles as they line up along the two-dimensional energy minimum. Hence, they allow for the separation of a larger number of particles per unit area than when using, e.g., periodic magnetic microstructures of circular shape.[11] The external field also reduces the formation of clusters of magnetic particles which is critical

for analysis, as particle clusters have larger magnetophoretic mobilities than the individual particles. The device can be used to separate magnetically labelled species from non-magnetic unlabelled species. It can also be used for the controlled transportation and mixing of biological and/or chemical species bound to magnetic particles without the need of fluid convection. Separation, for example, can be carried out as follows: First, a value of t_f is chosen above the threshold for transportation of beads that are not attached to the cells but below the threshold for transportation of beads that are attached to the cells. This will make it possible to remove all beads that are not bound to the cells. Subsequently, a higher value of t_f for which beads attached to the cells are transported can be chosen and the beads with cells are transported and collected. We envision the development of "magnetic chromatography," where different biological species labelled with particles having different magnetophoretic mobilities are separated in different areas of the device.

[1]R. Pethig, Biomicrofluidics **4**, 022811 (2010).
[2]M. A. M. Gijs, F. Lacharme, and U. Lehmann, Chem. Rev. **110**, 1518–1563 (2010).
[3]C.-P. Jen and W.-F. Chen, Biomicrofluidics **5**, 044105 (2010).
[4]I. Cheng, H.-C. Chang, D. Hou, and H.-C. Chang, Biomicrofluidics **1**, 021503 (2007).
[5]I.-F. Cheng, V. E. Froude, Y. Zhu, H.-C. Chang, and H.-C. Chang, Lab Chip **9**, 3193 (2009).
[6]G. Goet, T. Baier, and S. Hardt, Biomicrofluidics **5**, 014109 (2011).
[7]M. Donolato, M. Gobbi, P. Vavassori, M. Deryabina, M. F. Hansen, V. Metlushko, B. Ilic, M. Cantoni, D. Petti, S. Brivio, and R. Bertacco, Adv. Mater. **22**, 2706–2710 (2010).
[8]M. Donolato, A. Torti, E. Sogne, N. Kostesha, M. F. Hansen, and R. Bertacco, Lab Chip **11**, 2976–2983 (2011).
[9]K. Gunnarsson, P. E. Roy, S. Felton, J. Pihl, P. Svedlindh, S. Berner, H. Lidbaum, and S. Oscarsson, Adv. Mater. **17**, 1730 (2005).
[10]L.-E. Johansson, K. Gunnarsson, S. Bijelovic, K. Eriksson, A. Surpi, E. Göthelid, P. Svedlindh, and S. Oscarsson, Lab Chip **10**, 654–661 (2010).
[11]B. B. Yellen, R. M. Erb, H. S. Son, R. Hewlin, Jr., H. Shang, and G. U. Lee, Lab Chip **7**, 1681 (2007).
[12]L. Gao, N. J. Gottron III, L. N. Virgin, and B. Yellen, Lab Chip **10**, 2108 (2010).
[13]L. E. Helseth, T. M. Ficher, and T. H. Johansen, Phys. Rev. E **67**, 042401 (2003).
[14]A. Ehresmann, D. Lengemann, T. Weis, A. Albrecht, J. Langfahl-Klabes, F. Göllner, and D. Engel, Adv. Mater. **23**, 5568 (2011).
[15]A. Engel and R. Friedrichs, Am. J. Phys. **70**, 428 (2002).
[16]G. Fonnum, C. Johansson, A. Molteberg, S. Mørup, and E. Aksnes, J. Magn. Magn. Mater. **293**, 41–47 (2005).